African Journal of Mathematics and Statistics Studies
ISSN: 2689-5323
Volume 7, Issue 3, 2024 (pp. 143-155)
www.abjournals.org

MODELLING AND SIMULATION OF THE EFFECT OF PRANDTL AND SORET NUMBERS ON MASS CONCENTRATION WITH MAGNETIC INTENSITY IN A BLOOD CHANNEL

K. W. Bunonyo[1], J. K. Butter[2], and I. C. Eli[3]

[1,2,3]Department of Mathematics and Statistics, Federal University Otuoke, Ogbia, Bayelsa State, Nigeria.

[1,3]Mathematical Modelling and Data Analytics Research Group (MMDARG).

Cite this article:

K. W. Bunonyo, J. K. Butter, I. C. Eli (2024), Modelling and Simulation of the Effect of Prandtl and Soret Numbers on Mass Concentration with Magnetic Intensity in a Blood Channel. African Journal of Mathematics and Statistics Studies 7(3), 143-155. DOI: 10.52589/AJMSS-A7NIEBYY

Manuscript History

Received: 20 Jun 2024

Accepted: 26 Aug 2024

Published: 29 Aug 2024

ABSTRACT: *Mass concentration in blood is the amount of protein, glucose, and waste products present in a given blood volume, and the change in mass concentration can lead to several health challenges, such as cardiovascular problems. However, this research was focused on formulating a system of partial differential mathematical models that represent energy transfer in the blood and mass concentration. The models were further scaled to be dimensionless, reduced to ordinary differential equations using some perturbation conditions, and solved analytically using the Laplace method, where the temperature and mass concentration profiles were obtained. In addition, the numerical simulation was carried out using Wolfram Thematic, version 12, and the impact of the Prandtl and Soret numbers was investigated. The results indicate that the Prandtl number, Soret number, and many other numbers that appeared in the system were varied to understand the parameter changes on the profiles. Conclusion: We conclude that the oscillatory parameter and Prandtl number increased the temperature profiles, while other parameters increased the mass concentration as they increased.*

KEYWORDS: Mathematical Modelling, Thermosolutal, Blood, Flow, Magnetic, Field, Micro-channel.

Article DOI: 10.52589/AJMSS-A7NIEBYY
DOI URL: https://doi.org/10.52589/AJMSS-A7NIEBYY

African Journal of Mathematics and Statistics Studies
ISSN: 2689-5323
Volume 7, Issue 3, 2024 (pp. 143-155)

www.abjournals.org

Nomenclature

w^*, u^*	Dimensional blood velocity in different directions
x^*, r^*	Dimensional axial and radial distances
T^*	Dimensional blood temperature
T_∞	Far-field temperature of blood
c_{bp}	Blood specific heat capacity
ω	Oscillatory frequency
ϕ	Dimensionless Mass concentration profile
D_0	Diffusivity of the mass concentration
D_T	Diffusivity due to temperature
C^*	Dimensional mass concentration
C_∞	Far-field mass concentration
t	Dimensionless time
θ	Dimensionless temperature
k_{Tb}	Blood thermal conductivity
k_0	Chemical Reactant
Pr	Prandtl number
t	Dimensionless Time
Rd	Chemical reaction parameter
g	Acceleration due to gravity

Article DOI: 10.52589/AJMSS-A7NIEBYY
DOI URL: https://doi.org/10.52589/AJMSS-A7NIEBYY

African Journal of Mathematics and Statistics Studies
ISSN: 2689-5323
Volume 7, Issue 3, 2024 (pp. 143-155)

www.abjournals.org

INTRODUCTION

Blood circulation is a continuous loop that delivers oxygen and nutrients to cells while removing waste Athani *et al.* (2022). The heart pumps oxygenated blood through arteries, which branch into tiny capillaries for exchange. Deoxygenated blood travels through veins back to the heart for re-oxygenation in the lungs Bunonyo & Ebiwareme (2022). Blood vessel narrowing, called stenosis makes it much harder for blood to flow properly. This disrupts blood circulation and heart function. Plaque buildup, a combination of cholesterol and cells, causes the narrowing. The narrower the vessel, the less oxygen-rich blood can get through, raising the risk of heart failure Kubugha & Amos (2022). This narrowing doesn't just affect the amount of blood flow; it also changes the pressure and speed of blood flow throughout the vessel Yusuf *et al.* (2016). Bunonyo and Ebiwareme (2024) investigated the two-dimensional magneto-hydrodynamics laminar flow of a Sisko nanofluid over a nonlinear stretching sheet in a porous medium, considering chemical reactions, the nonlinear Rosseland approximation, and an internal heat source-based on concentration. Yadav and Roshan (2024) investigated the electromagnet hydrodynamic peristaltic flow of blood through the annulus between two concentric circular tubes, aiming to advance peristaltic endoscope technology. Sharma *et al.* (2023) presented a Magneto-hydrodynamics haemodynamics hybrid nanofluid flow through an inclined stenotic artery. Kumawat *et al.* (2021) presented a mathematical analysis of two-phase blood flow through a stenosed curved artery with haematocrit and temperature-dependent viscosity. Shah *et al.* (2021) discussed the effects of pulsatile pressure gradient in the presence of a transverse magnetic field on unsteady blood flow through an inclined tapered cylindrical tube of porous medium. Selvi *et al.* (2021) proposed a theoretical model to investigate the coupled effects of thermal radiation and electromagnetic field on the blood flow in a stenosed tapered artery. Fahim et al. (2024) presented a computational analysis of a Pulsatile pressure-driven non-Newtonian blood flow through a porous stenotic artery using the Navier-Stokes equations and the Carreau fluid model to represent blood rheology. Mamun *et al.* (2020) looked into the influence of a magnetic field on blood flow via a stenotic artery. Ferro-fluids were employed for a variety of purposes, including magnetic separation, anticancer medication delivery, and micro-valves. The research conducted by Priyadharsini (2023) focuses on the mathematical modelling and analysis of the impact of thermoregulation on blood viscosity under magnetic and thermal radiation effects in a porous, stretching blood capillary. The investigation conducted by Hosseinzadeh *et al.* (2022) focused on the study of non-Newtonian blood fluid flow containing nanoparticles within a vessel with a porous wall, in the presence of a magnetic field. Verma & Parihar (2010) developed a mathematical model of blood flow through a tapered artery with mild stenosis and haematocrit. However, the Verma and Parihar research couldn’t go further in investigating the effect of the heat on the velocity profile and Bunonyo others didn’t study further on the effect of heat on mass concentration and the mass concentration on the blood flow profile, which this study aims to achieve.

Article DOI: 10.52589/AJMSS-A7NIEBYY
DOI URL: https://doi.org/10.52589/AJMSS-A7NIEBYY

African Journal of Mathematics and Statistics Studies
ISSN: 2689-5323
Volume 7, Issue 3, 2024 (pp. 143-155)

www.abjournals.org

Mathematical Formulation

Before we begin developing a system of mathematical models representing the thermosolutal effect on blood flow through a microchannel, consider the following realistic assumptions: The flow is axial; the tangential velocity is assumed to be zero; the fluid is blood, incompressible, and viscous; the viscosity is constant throughout the fluid medium; the flow could be driven by the thermosolutal effect; there is no electrical conductivity in the system; we considered the effect of an external magnetic field; and the blood vessel is porous; the flow obeys the no-slip condition. The mathematical model system is presented based on the assumptions made above and previous research by Bunonyo et al. (2018), Bunonyo and Amos (2023), Hanvey & Bunonyo (2022), and Verma and Parihar (2010).

Energy Equation

Following Bunonyo *et al*. (2018), the energy equation is:

$$\rho_b c_{bp} \frac{\partial T^*}{\partial t^*} = k_{Tb}\left(\frac{\partial^2 T^*}{\partial r^{*2}} + \frac{1}{r^*}\frac{\partial T^*}{\partial r^*}\right) \tag{1}$$

Mass Concentration Equation

Following Bunonyo *et al*. (2021), the mass concentration equation is

$$\frac{\partial C^*}{\partial t^*} = D_0\left(\frac{\partial^2 C^*}{\partial r^{*2}} + \frac{1}{r^*}\frac{\partial C^*}{\partial r^*}\right) - k_0\left(C^* - C_\infty\right) + \frac{D_T k_{Tb}}{T_m}\left(\frac{\partial^2 T^*}{\partial r^{*2}} + \frac{1}{r^*}\frac{\partial T^*}{\partial r^*}\right) \tag{2}$$

The corresponding boundary conditions are:

$$\left.\begin{aligned} T^* = T_w, C^* = C_w \quad \text{at } r^* = R < \infty \\ T^* \neq T_w, C^* \neq C_w \quad \text{at } r^* = 0 \end{aligned}\right\} \tag{3}$$

Dimensionless Quantities

$$\left.\begin{aligned} x^* = x\lambda, r^* = rR_0, \upsilon_b = \frac{\mu_b}{\rho_b}, t^* = \frac{R_0^2 t}{\upsilon_b}, Sr = \frac{D_T k_{Tb}\left(T_w - T_\infty\right)}{D_0 T_m\left(C_w - C_\infty\right)}, \\ \theta = \frac{T^* - T_\infty}{T_w - T_\infty}, \phi = \frac{C^* - C_\infty}{C_w - C_\infty}, Pr = \frac{\mu_b c_{bp}}{k_{Tb}}, Sc = \frac{D_0}{\upsilon_b}, Rd = \frac{k_0 R_0^2}{D_0} \end{aligned}\right\} \tag{4}$$

Simplifying equations (1)-(3), using equation (4), we have:

$$Pr\frac{\partial \theta}{\partial t} = \frac{\partial^2 \theta}{\partial r^2} + \frac{1}{r}\frac{\partial \theta}{\partial r} \tag{5}$$

Article DOI: 10.52589/AJMSS-A7NIEBYY
DOI URL: https://doi.org/10.52589/AJMSS-A7NIEBYY

African Journal of Mathematics and Statistics Studies
ISSN: 2689-5323
Volume 7, Issue 3, 2024 (pp. 143-155)

$$\frac{\partial \phi}{\partial t} = Sc\left(\frac{\partial^2 \phi}{\partial r^2} + \frac{1}{r}\frac{\partial \phi}{\partial r}\right) - RdSc\phi + SrSc\left(\frac{\partial^2 \theta}{\partial r^2} + \frac{1}{r}\frac{\partial \theta}{\partial r}\right) \tag{6}$$

The corresponding boundary conditions are:

$$\left.\begin{array}{ll} \theta = 1, \phi = 1, & \text{at } r = h < \infty \\ \theta \neq 0, \phi \neq 0, & \text{at } r = 0 \end{array}\right\} \tag{7}$$

Perturbation Solution

Since the fluid motion is a function of the pumping action of the heart, we consider the solution to be in the following form:

$$\left.\begin{array}{l} \theta = \theta_0 e^{\omega t} \\ \phi = \phi_0 e^{\omega t} \end{array}\right\} \tag{8}$$

We can reduce equations (5), (6), and equation (7) using equation (8), which is:

$$r\frac{d^2\theta_0}{dr^2} + \frac{d\theta_0}{dr} - \lambda_2^2 r\theta_0 = 0 \tag{9}$$

$$r\frac{d^2\phi_0}{dr^2} + \frac{d\phi_0}{dr} - \lambda_3^2 r\phi_0 + Sr\left(r\frac{d^2\theta_0}{dr^2} + \frac{d\theta_0}{dr}\right) = 0 \tag{10}$$

$$\left.\begin{array}{ll} \theta_0 = e^{-\omega t}, \phi_0 = e^{-\omega t}, & \text{at } r = h < \infty \\ \theta_0 \neq 0, \theta_0 \neq 0, & \text{at } r = 0 \end{array}\right\} \tag{11}$$

where: $\lambda_2^2 = Pr\omega$ and $\lambda_3^2 = \left(Rd + \frac{\omega}{Sc}\right)$

Method of Solution

The Laplace transform for the energy and concentration functions can be stated as:

$$\left.\begin{array}{l} L\{\theta_0(r)\} = \theta_0(s) = \int_0^\infty \theta_0(r) e^{-sr} dr \\ L\{\phi_0(r)\} = \phi_0(s) = \int_0^\infty \phi_0(r) e^{-sr} dr \end{array}\right\} \tag{12}$$

The equations (9) and (10) can be solved using the Laplace method in equation (12), the solutions is:

Article DOI: 10.52589/AJMSS-A7NIEBYY
DOI URL: https://doi.org/10.52589/AJMSS-A7NIEBYY

African Journal of Mathematics and Statistics Studies
ISSN: 2689-5323
Volume 7, Issue 3, 2024 (pp. 143-155)
www.abjournals.org

$$\left(s^2 - Pr\omega\right)\frac{d\theta_0}{ds} = -s\theta_0\left(s\right) \tag{13}$$

where $\lambda_2^2 = Pr\omega$

Further simplification of equation (13), we have:

$$\theta_0\left(s\right) = \frac{A}{\sqrt{\left(s^2 - \lambda_2^2\right)}} \tag{14}$$

We know that: $\theta_0\left(r\right) = L^{-1}\left\{\theta_0\left(s\right)\right\}$, therefore, solving equation (14) gives;

$$\theta_0\left(r\right) = AI_0\left(\lambda_2 r\right) \tag{15}$$

where $I_0\left(\lambda_2 r\right)$ is the modified Bessel function of order zero.

Solving equation (15) using the boundary conditions in equation (11), we have:

$$A = \frac{1}{I_0\left(\lambda_2 h\right)e^{\omega t}} \tag{16}$$

Putting equation (16) into equation (15) gives:

$$\theta_0\left(r\right) = \frac{I_0\left(\lambda_2 r\right)}{I_0\left(\lambda_2 h\right)e^{\omega t}} \tag{17}$$

where

$$I_0\left(\lambda_2 r\right) = \left(1 + \frac{\lambda_2^2 r^2}{4} + \frac{\lambda_2^4 r^4}{64} + \frac{\lambda_2^6 r^6}{2304} + ...\right) \text{ and } I_0\left(h\lambda_2\right) = \left(1 + \frac{h^2\lambda_2^2 r^2}{4} + \frac{h^4\lambda_2^4 r^4}{64} + \frac{h^6\lambda_2^6 r^6}{2304} + ...\right)$$

Substituting equation (17) into equation (8), we have:

$$\theta\left(r\right) = \frac{1}{I_0\left(\lambda_2 h\right)}\left(1 + \frac{\lambda_2^2 r^2}{4} + \frac{\lambda_2^4 r^4}{64} + \frac{\lambda_2^6 r^6}{2304} + ...\right) \tag{18}$$

Substituting equation (18) into the mass concentration equation (10), we get:

$$\frac{d^2\phi_0}{dr^2} + \frac{1}{r}\frac{d\phi_0}{dr} - \lambda_3^2\phi_0 = -\frac{\lambda_2^2 Sr}{I_0\left(\lambda_2 h\right)e^{\omega t}}\left(1 + \frac{\lambda_2^2 r^2}{4} + \frac{\lambda_2^4 r^4}{64}\right) \tag{19}$$

Presenting equation (19) with a particular term, we have:

$$r\frac{d^2\phi_{0p}}{dr^2} + \frac{d\phi_{0p}}{dr} - \lambda_3^2 r\phi_{0p} = -\frac{\lambda_2^2 Sr}{I_0\left(\lambda_2 h\right)e^{\omega t}}\left(r + \frac{\lambda_2^2 r^3}{4} + \frac{\lambda_2^4 r^5}{64}\right) \tag{20}$$

Article DOI: 10.52589/AJMSS-A7NIEBYY
DOI URL: https://doi.org/10.52589/AJMSS-A7NIEBYY

African Journal of Mathematics and Statistics Studies
ISSN: 2689-5323
Volume 7, Issue 3, 2024 (pp. 143-155)
www.abjournals.org

The particular solution of equation (20) can be presented as:

$$\phi_{0p} = A_0 + A_1 r + A_2 r^2 + A_3 r^3 + A_4 r^4 + A_5 r^5 \tag{21}$$

Solving equation (20), we have:

$$\left.\begin{aligned} A_0 &= \frac{Sr}{I_0(\lambda_2 h)e^{\omega t}}\left\{\frac{\lambda_2^2}{\lambda_3^2}+\frac{\lambda_2^4}{\lambda_3^4}+\frac{\lambda_2^6}{\lambda_3^6}\right\},\ A_1 = 0, \\ A_2 &= \frac{Sr}{4I_0(\lambda_2 h)e^{\omega t}}\left\{\frac{\lambda_2^4}{\lambda_3^2}+\frac{\lambda_2^6}{\lambda_3^4}\right\}, A_3 = 0, \\ A_4 &= \frac{\lambda_2^6}{64\lambda_3^2}\frac{Sr}{I_0(\lambda_2 h)e^{\omega t}}, A_5 = 0, \end{aligned}\right\} \tag{22}$$

Substituting equation (22) into equation (21), we have:

$$\phi_{0p} = \frac{Sr}{I_0(\lambda_2 h)e^{\omega t}}\left\{\frac{\lambda_2^2}{\lambda_3^2}+\frac{\lambda_2^4}{\lambda_3^4}+\frac{\lambda_2^6}{\lambda_3^6}\right\} + \frac{Sr}{4I_0(\lambda_2 h)e^{\omega t}}\left\{\frac{\lambda_2^4}{\lambda_3^2}+\frac{\lambda_2^6}{\lambda_3^4}\right\} r^2 + \frac{\lambda_2^6}{64\lambda_3^2}\frac{Sr}{I_0(\lambda_2 h)e^{\omega t}} r^4 \tag{23}$$

The homogeneous solution of equation (20) is:

$$\phi_{0h} = c_2 I_0(\lambda_3 r) \tag{24}$$

The general solution of equation (20) is the sum of the homogeneous equation (24) and equation (23), which is:

$$\phi_0 = c_2 I_0(\lambda_3 r) + \frac{Sr}{I_0(\lambda_2 h)e^{\omega t}}\left\{\frac{\lambda_2^2}{\lambda_3^2}+\frac{\lambda_2^4}{\lambda_3^4}+\frac{\lambda_2^6}{\lambda_3^6}\right\} + \frac{Sr}{4I_0(\lambda_2 h)e^{\omega t}}\left\{\frac{\lambda_2^4}{\lambda_3^2}+\frac{\lambda_2^6}{\lambda_3^4}\right\} r^2 + \frac{\lambda_2^6}{64\lambda_3^2}\frac{Sr}{I_0(\lambda_2 h)e^{\omega t}} r^4 \tag{25}$$

Using the boundary conditions in equation (11), we get:

$$c_2 = \left\{\begin{aligned} &\frac{e^{-\omega t}}{I_0(\lambda_3 h)} - \frac{Sr}{I_0(\lambda_2 h)I_0(\lambda_3 h)e^{\omega t}}\left\{\frac{\lambda_2^2}{\lambda_3^2}+\frac{\lambda_2^4}{\lambda_3^4}+\frac{\lambda_2^6}{\lambda_3^6}\right\} - \frac{Sr}{4I_0(\lambda_2 h)I_0(\lambda_3 h)e^{\omega t}}\left\{\frac{\lambda_2^4}{\lambda_3^2}+\frac{\lambda_2^6}{\lambda_3^4}\right\} h^2 \\ &-\frac{\lambda_2^6}{64\lambda_3^2}\frac{Sr}{I_0(\lambda_2 h)I_0(\lambda_3 h)e^{\omega t}} h^4 \end{aligned}\right\} \tag{26}$$

Therefore, equation (25) becomes:

$$\phi_0 = c_2 I_0(\lambda_3 r) + A_0 + A_1 r^2 + A_2 r^4 \tag{27}$$

Article DOI: 10.52589/AJMSS-A7NIEBYY
DOI URL: https://doi.org/10.52589/AJMSS-A7NIEBYY

African Journal of Mathematics and Statistics Studies
ISSN: 2689-5323
Volume 7, Issue 3, 2024 (pp. 143-155)
www.abjournals.org

where

$$A=\frac{Gr}{I_0(\lambda_2 h)},A_0=\frac{SrGc}{I_0(\lambda_2 h)e^{\omega t}}\left\{\frac{\lambda_2^2}{\lambda_3^2}+\frac{\lambda_2^4}{\lambda_3^4}+\frac{\lambda_2^6}{\lambda_3^6}\right\},A_1=\frac{SrGc}{4I_0(\lambda_2 h)e^{\omega t}}\left\{\frac{\lambda_2^4}{\lambda_3^2}+\frac{\lambda_2^6}{\lambda_3^4}\right\},A_2=\frac{\lambda_2^6}{64\lambda_3^2}\frac{SrGc}{I_0(\lambda_2 h)e^{\omega t}}$$

PRESENTATION OF RESULTS

After proffering analytical solutions to the formulated problem, numerical simulation using Wolfram Mathematica version 12 was performed and in order to validate the analytical solution, the parameters data were obtained from previous research carried out by Bunonyo and Amos (2023), Bunonyo *et al*. (2021), and Hanvey and Bunonyo (2022), respectively. The results are presented as Figure1 to Figure 5,:

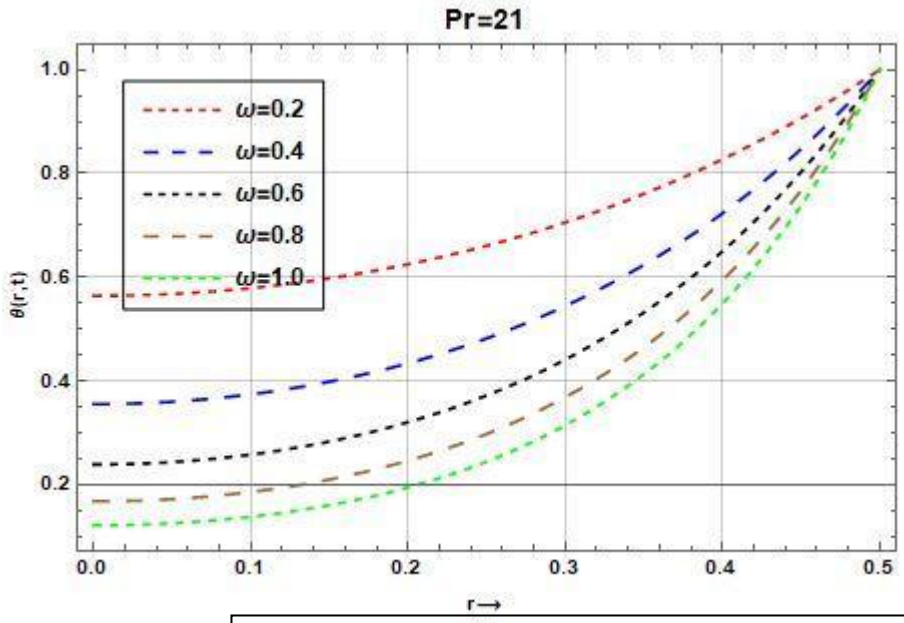

Figure 1 The effect of oscillation on the fluid temperature

Article DOI: 10.52589/AJMSS-A7NIEBYY
DOI URL: https://doi.org/10.52589/AJMSS-A7NIEBYY

African Journal of Mathematics and Statistics Studies
ISSN: 2689-5323
Volume 7, Issue 3, 2024 (pp. 143-155)
www.abjournals.org

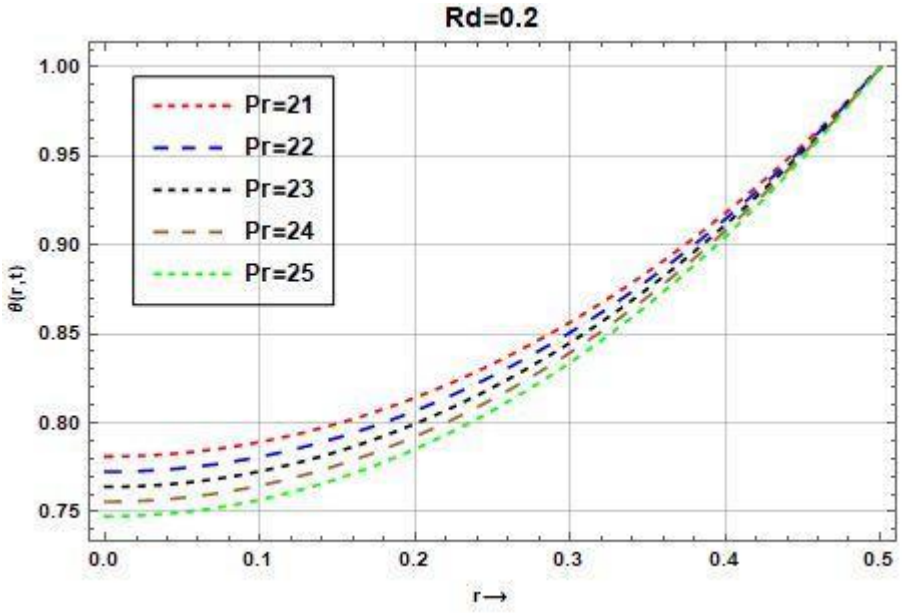

Figure 2 The effect of Prandtl number on the fluid temperature

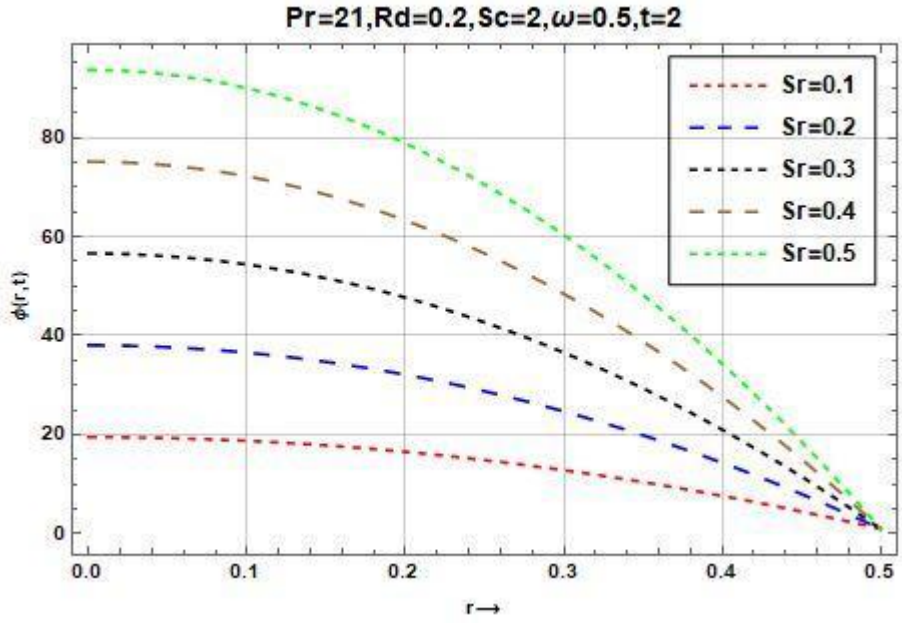

Figure 3 The effect of Soret number on mass concentration

Article DOI: 10.52589/AJMSS-A7NIEBYY
DOI URL: https://doi.org/10.52589/AJMSS-A7NIEBYY

African Journal of Mathematics and Statistics Studies
ISSN: 2689-5323
Volume 7, Issue 3, 2024 (pp. 143-155)
www.abjournals.org

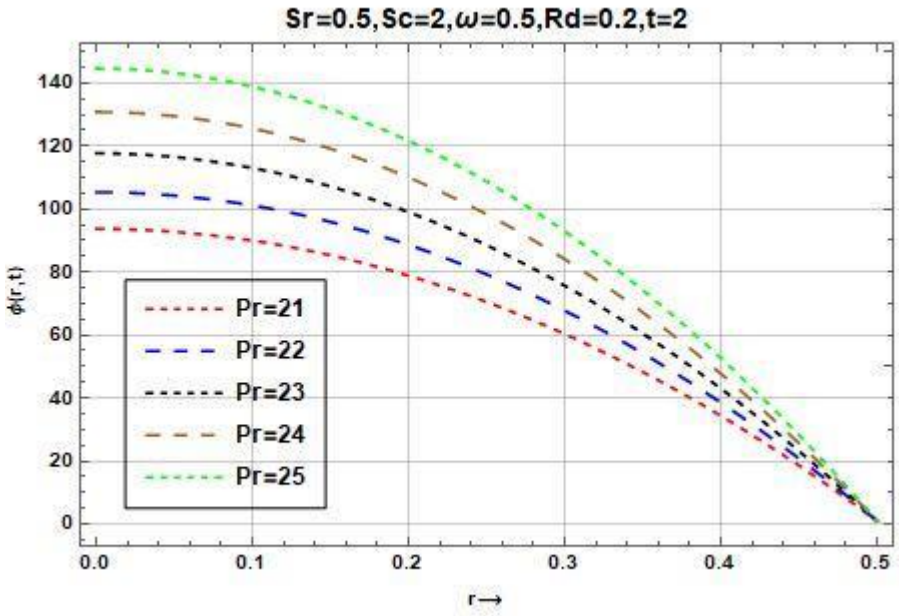

Figure 4 The effect of Prandtl number on mass concentration

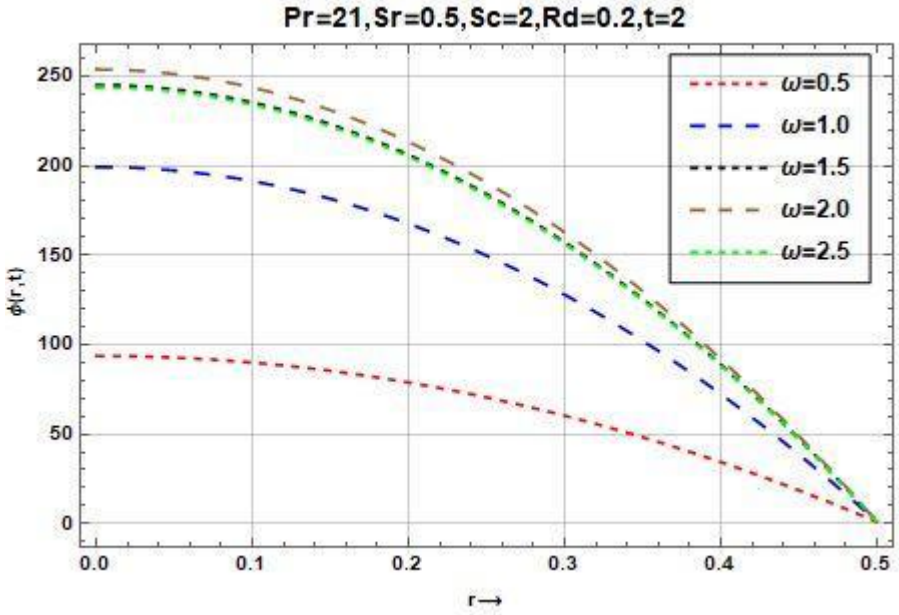

Figure 5 The effect of oscillatory number on mass concentration

Article DOI: 10.52589/AJMSS-A7NIEBYY
DOI URL: https://doi.org/10.52589/AJMSS-A7NIEBYY

African Journal of Mathematics and Statistics Studies
ISSN: 2689-5323
Volume 7, Issue 3, 2024 (pp. 143-155)

www.abjournals.org

DISCUSSION OF RESULTS

It's observed in Figure 1 that the temperature profile increases along the boundary for the Prandtl number $Pr = 21$ and the oscillatory frequency at $\omega = 0.2$. However, the profile showed a decrease in temperature profile for the increasing values of the oscillatory frequency $\omega = 0.2, 0.4, 0.6, 0.8, 1.0$ before converging to 1 as the boundary layer attains its peak of 0.5. We can also observe in Figure 2 that the temperature profile increases along the boundary for the chemical reaction parameter $Rd = 0.2$ and the Prandtl number at $Pr = 21$. However, the profile indicates a decrease in temperature profile though much slower than that of increasing oscillatory frequency, for the increasing values of the Prandtl number $Pr = 21, 22, 23, 24, 25$ before converging to 1 as the boundary layer attains its peak of 0.5. Figure 3 shows that the mass concentration profile decreases along the boundary layer where other pertinent parameters are considered as $Rd = 0.2, Sc = 0.2, \omega = 0.5, , Pr = 21, t = 2$ and the Soret number at $Sr = 0.1$. However, it can be seen in the figure that the mass concentration continuously decreased for different rates of increase of the Soret number $Sr = 0.2, 0.4, 0.6, 0.8, 1.0$ before converging to 0 as the boundary layer attained its maximum value of 0.5. Figure 4 shows that the mass concentration profile increases along the boundary layer thickness where other pertinent parameters are considered as $Rd = 0.2, Sc = 0.2, \omega = 0.5, Sr = 0.1, t = 2$ and the Prandtl number at $Pr = 21$. The observation in the figure is of the view that the mass concentration slowly increases for different values of the Prandtl number $Pr = 21, 22, 23, 24, 25$ before converging to 0 as the boundary layer attains its maximum value of 0.5.

Figure 5 shows that the mass concentration profile increases along the boundary layer thickness where other pertinent parameters are considered as $Rd = 0.2, Sc = 0.2, Pr = 21, Sr = 0.5, t = 2$ and the oscillatory frequency of $\omega = 0.5$. The observation indicates that the mass concentration slowly increases for different values of the oscillatory frequency $\omega = 0.5, 1.0, 1.5, 2.0, 2.5$ before converging to 0 as the boundary layer thickness grows to 0.5.

CONCLUSION

Following the modelling and analysis of the thermal impact on the mass concentration in blood in a blood vessel, we performed numerical simulation and the results were discussed extensively and we conclude as follows:

1. The increase in oscillatory frequency decreases the temperature of the fluid in the vessel
2. The Prandtl number impacted the fluid because the increase in the Prandtl number caused a corresponding decrease in fluid temperature in the channel.
3. The Soret number also affected the mass concentration of the fluid because an increase in the Soret number also increased the mass concentration in the channel.
4. The increase in Prandtl number increases the mass concentration in the channel.

Article DOI: 10.52589/AJMSS-A7NIEBYY
DOI URL: https://doi.org/10.52589/AJMSS-A7NIEBYY

5. An increase in the oscillatory frequency also increases the mass concentration in the fluid.

CONFLICT OF INTEREST

The authors declare no conflict of interest

REFERENCES

Athani, A., Ghazali, N. N. N., Badruddin, I. A., Kamangar, S., Anqi, A. E., &Algahtani, A. (2022). Investigation of two-way fluid-structure interaction of blood flow in a patient-specific left coronary artery. *Bio-Medical Materials and Engineering*, *33*(1), 13-30

Bunonyo, K. W., & Ebiwareme, L. (2022). A low Prandtl number haemodynamic oscillatory flow through a cylindrical channel using the Power Series Method. European Journal of Applied Physics, 4(3), 56-65.

Bunonyo, K. W., Amos, E., & Eli, I. C. (2018). Unsteady oscillatory couette flow between vertical parallel plates with constant radiative heat flux. *Asian Research Journal of Mathematics*, *11*(2), 1-11.

Bunonyo, K. W., & Amos, E. (2020). Lipid concentration effect on blood flow through an inclined arterial channel with magnetic field. *Mathematical modelling and Applications*, *5*(3), 129.

Bunonyo, K. W., Amos, E., & Nwaigwe, C. (2021). Modeling the treatment effect on LDL-C and atherosclerotic blood flow through microchannel with heat and magnetic field. *International Journal of Mathematics Trends and Technology-IJMTT*, *67*.

Bunonyo, K. W., & Amos, E. (2022). Convective Flow of Blood through a Constricted Cylinder and the Effect of Cholesterol Growth Rate on the Motion in the Presence of a Magnetic Field. *African Scientific Reports*, 174-187.

Ebiwareme, L., & Bunonyo, K. W. (2024). Chemical Reaction and Nonlinear Rosseland Approximation Effects On Double-Diffusive MHD Sisko Nanofluid Flow Over a Nonlinear Stretching Sheet in A Porous Medium with Concentration-Dependent Internal Heat Source. British Journal of Multidisciplinary and Advanced Studies, 5(1), 1-20.

Fahim, M., Sajid, M., & Ali, N. (2024). Pulsatile pressure-driven non-Newtonian blood flow through a porous stenotic artery: A computational analysis. Numerical Heat Transfer, Part A: Applications, 1-21.

Gul, T., Nasir, S., Berrouk, A. S., Raizah, Z., Alghamdi, W., Ali, I., & Bariq, A. (2023). Simulation of the water-based hybrid nanofluids flow through a porous cavity for the applications of the heat transfer. *Scientific Reports*, *13*(1), 7009.

Hosseinzadeh, S., Hosseinzadeh, K., Hasibi, A., & Ganji, D. D. (2022). Hydrothermal analysis on non-Newtonian nanofluid flow of blood through porous vessels. Proceedings of the Institution of Mechanical Engineers, Part E: Journal of Process Mechanical Engineering, 236(4), 1604-1615.

Kubugha, B. W., & Amos, E. (2022). Mathematical Modeling of LDL-C and Blood Flow through an Inclined Channel with Heat in the Presence of Magnetic Field. Trends in Sciences, 19(16), 5693-5693.

Article DOI: 10.52589/AJMSS-A7NIEBYY
DOI URL: https://doi.org/10.52589/AJMSS-A7NIEBYY

Hanvey, R. R., & Bunonyo, K. W. (2022). Effect of treatment parameter on oscillatory flow of blood through an atherosclerotic artery with heat transfer. *Journal of the Nigerian Society of Physical Sciences*, 682-682.

Kumawat, C., Sharma, B. K., &Mekheimer, K. S. (2021). Mathematical analysis of two-phase blood flow through a stenosed curved artery with hematocrit and temperature dependent viscosity. Physica Scripta, 96(12), 125277.

Mamun, K., Funazaki, K., Akter, S., & Akhter, M. N. (2020). The effect of magnetic field on blood flow through stenotic artery-a review on bio-magnetic fluid dynamics. Series on Biomechanics, 34(1), 20-30.

Priyadharsini, M. (2023). Mathematical modelling and analysis of thermoregulation effects on blood viscosity under magnetic effects and thermal radiation in a permeable stretching capillary. Journal of Thermal Biology, 111, 103398.

Selvi, R. T., Ponalagusamy, R., & Padma, R. (2021). Influence of electromagnetic field and thermal radiation on pulsatile blood flow with nanoparticles in a constricted porous artery. International Journal of Applied and Computational Mathematics, 7, 1-25.

Shah, N. A., Al-Zubaidi, A., & Saleem, S. (2021). Study of Magnetohydrodynamic Pulsatile Blood Flow through an Inclined Porous Cylindrical Tube with Generalized Time-Nonlocal Shear Stress. *Advances in Mathematical Physics*, *2021*(1), 5546701.

Sharma, B. K., Gandhi, R., Abbas, T., & Bhatti, M. M. (2023). Magnetohydrodynamics hemodynamics hybrid nanofluid flow through inclined stenotic artery. Applied Mathematics and Mechanics, 44(3), 459-476.

Verma, N., & Parihar, R. S. (2010). Mathematical model of blood flow through a tapered artery with mild stenosis and hematocrit. J. Mod. Math. Stat, 4(1), 38-43.

Yadav, P. K., & Roshan, M. (2024). Mathematical modeling of blood flow in an annulus porous region between two coaxial deformable tubes: An advancement to peristaltic endoscope. *Chinese Journal of Physics*, *88*, 89-109.

Yusuf, S., Lonn, E., Pais, P., Bosch, J., López-Jaramillo, P., Zhu, J. ... & Parkhomenko, A. (2016). Blood-pressure and cholesterol lowering in persons without cardiovascular disease. New England Journal of Medicine, 374(21), 2032-2043.

Article DOI: 10.52589/AJMSS-A7NIEBYY
DOI URL: https://doi.org/10.52589/AJMSS-A7NIEBYY